# The DSC Thermal Analysis of Crystallization Behavior in Palm Oil[1]

K. KAWAMURA,[1], Knorr Foods Co., Ltd.,
Takatsu-ku, Kawasaki-shi, Japan

## ABSTRACT

Polymorphic behavior of palm oil crystals was studied by DSC isothermal analysis and microscopic observation. Different crystal forms developed specific spherulites depending on the degree of supercooling from the melt. The A-form crystal was capable of forming a dotted spherulite and the B-form crystal of forming a dendritic spherulite. Experimental results of B form crystallization studied by the DSC and a microscope under kinetic conditions were evaluated using Avarami's theory, since the behavior of the oil during crystallization related well to that of high polymers. The crystallization process was divided into nucleation and crystal-growth phases to facilitate a theoretical treatment similar to that of high polymers, providing crystals possessing overall structural regularity.

## INTRODUCTION

Oil crystals have been previously analyzed for their polymorphic behavior using X-ray diffraction, thermoanalytic methods, etc., but some kinetic aspects like crystal growth have yet to be explained (1-9). However, some researchers have made significant progress toward explaining these aspects (10,11).

It could be supposed in a broad sense that oils behave like high polymers when subjected to the crystallization processes from the melt, i.e., they pass through the stages of nucleation, activation, crystal growth and finally reach the end state of a crystal lattice (12). The crystallization process is the spontaneous ordering of the system — the partial or complete restriction of motion in which triglyceride molecules are being linked with each other by chemical or physical bonds. Differences in crystal forms are the result of different molecular packings (13-15). Hoerr (16) has investigated polymorphism and suggested that it influences the growth of crystal spherulites resulting in different physical properties of crystal forms. Under isothermal conditions, crystals of palm oil are composed of A- and B- forms. A- and B- forms are only used as tentative terms in this report. A form crystals are transformed to the other form under isothermal conditions or during the heating process, e.g., at a rate of 10°K/min., but B-form crystals are stable. The spherulites are shown under a microscope to be identified with these different crystal forms, and the predominant one is dependent on the condition of supercooling.

This paper also attempts to clarify aspects of crystal growth of the B-form in palm oil. The crystallization follows the two main phases of nucleation and crystal growth, but it is very hard to separate them. Theoretically, it is possible to consider these processes relative to crystallization kinetics in high polymers. The theory was initially constructed on low molecular weight materials such as metals by Avrami (17-19) and Evans (20), the base of which was related to the theory of water droplet formation by Volmer et al. (21). It was extended to the crystallization of high polymers by Mandelkern et al. (22,23). These methods were also developed by Takayanagi et al. (24-28) with poly-(ethylene succinate) and poly-(ethylene adipate); by Barnes et al. (29) with poly-(ethylene oxide); and by Kamide et al. (30,31) with isotactic polypropylene.

Barnes' (29) and Takayanagi's analytical methods (24-28) are probably best suited to the case of palm oil crystallization. The triglyceride molecules are combined to form embryos by collision with each other and/or with foreign particles in the supercooled melt of palm oil. When they are charged with a certain activation energy which exceeds a critical level for nucleation, they initiate crystal growth. The crystal growth is composed of surface nucleation and molecular transportation (diffusion), i.e., more molecules are transported to adhere to surface nuclei on spherulites. Daughter crystals are constantly nucleated on the surface of parent spherulites and finally cover them to link with adjacent daughter crystals.

Unless polymorphic changes occur, the crystallization which passes through the above process seems to depend on supercooling, which is defined as the difference between the crystallization temperature (T), and the melting point (Tm), by DSC analysis.

## EXPERIMENTAL PROCEDURE

### Materials

The sample oil was a commercially available whole palm oil from Malaysia with a 54.5 iodine value and with the following fatty acid composition (32): 43.0% of C16:0, 4.5% of C18:0, 39.5% of C18:1 and 11.5% of C18:2. The sample was filtered with a membrane filter (Nalgene Filter Unit: 0.20 micron) to eliminate dust and other foreign particles.

### DSC Thermal Method

A Perkin Elmer Model DSC-2 was used. A piece of polyethylene terephthalate (12 mg) was sealed in an aluminum sample pan with a lid and used as a reference. Oil samples of ca. 9 mg were also sealed in sample pans and held at 393°K for more than 5 min to destroy crystal nuclei before each DSC scan. The temperature was rapidly dropped under maximum programmed conditions (ca. -80°K/min.) and held at the desired temperature (291°K to 305°K) for the isothermal crystallization. The starting point was defined as the time when the indicating (green)

TABLE I

The Constant "n" and "z," Defined by Avrami's Equation, Which Are Due to the Relation between the Nucleation and the Spherulite Growth[a]

| Mechanism of crystal growth | Nucleation sporadic in time | | Nucleation predetermined | |
|---|---|---|---|---|
| | n | z | n | z |
| Polyhedral | 4 | $\pi G^3 I/3$ | 3 | $4\pi G^3 I'/3$ |
| Plate-like | 3 | $\pi G^2 I/3$ | 2 | $\pi G^2 I'$ |
| Linear | 2 | $\pi d^2 G I/r$ | 1 | $\pi d^2 G I'/2$ |

[a]G: Linear growth rate of crystal-spherulite; I: sporadic nucleation rate in time; I': density of the primary nuclei in the pre-determined nucleation; d: width of fibril; n: constant in Avrami's equation; z: rate constant in Avrami's equation.

[1] Present address: Best Foods Research Center, Division of CPC International Inc., Union, New Jersey 07083

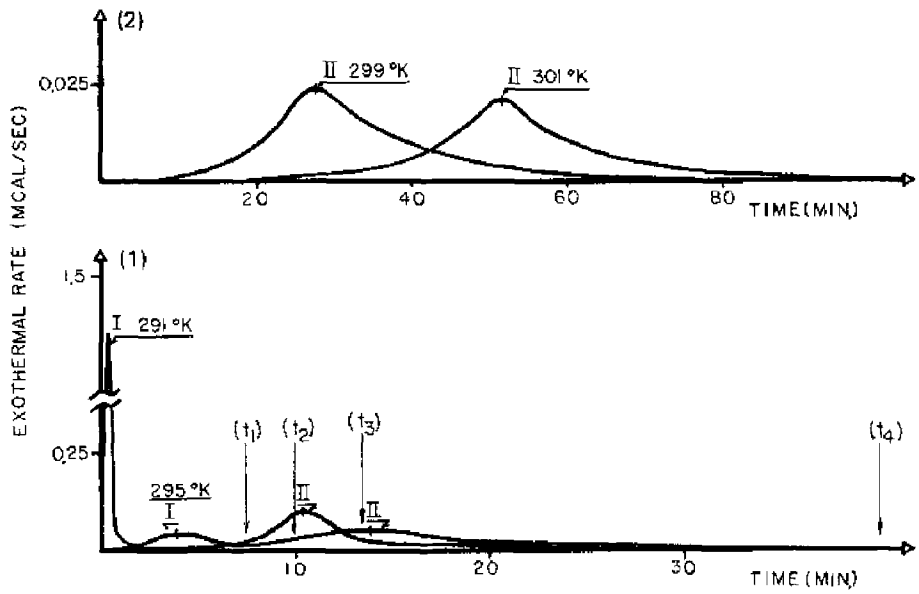


FIG. 1. DSC isothermal crystallization curves of palm oil. Exothermal rate (mcal/sec) vs. time in min at various temperatures between 291 and 301°K. 1) Crystallization temperature below 297°K. Two exothermal peaks -I, -II. 2) Crystallization temperature of 299°K or higher. One exothermal peak -II.

lamp lit on the DSC front panel, which meant the system was under temperature control. The generated crystals were then heated from that temperature (291 to 305°K) at a constant rate of 10°K/min. or 40°K/min. to obtain the DSC heating curves. The peak temperature (°K) was obtained from DSC heating curves and used for determination of crystal forms.

The bulk crystallization rate was calculated from the DSC isothermal crystallization curves. The area enclosed by a base line and an exothermal peak corresponds to the heat of crystallization, $\Delta H$. The fraction of crystals (C) at a given time (t) was approximated by the ratio of the integration of the exothermal rate, $\int d\Delta H(t)/dt$, to the total area, $\Delta H$, in accordance with the following equation.

$$C = \left(\int_{t=o}^{t} \frac{d\Delta H(t)}{dt} \cdot dt\right)/\Delta H \qquad (I)$$

The equation developed by Avrami (17-19) and Evans (20) was:

$$1 - C = \exp(-z \cdot t^n) \qquad (II)$$

where z was the rate constant of crystallization and n was the constant defined in accordance with the mechanism of crystallization. The relationship between z and n was derived from the mechanism of nucleation and the morphology of spherulite growth, as designated in Table I.

Equation (II) can be converted to (III):

$$\log(-\log(1-C)) = \log(z/2.3) + n \cdot \log t \qquad (III)$$

The constant terms of log (z/2.3) and n can be determined from a linear equation of the relationship between log (- log (1-C)) and log t. Therefore, as the relationship between C and t was calculated from the DSC isothermal crystallization curves of palm oil, the kinetics of oil crystallization could be represented by equation (II).

### Microscopic Observation

Oil crystals were observed under a microscope for their morphological changes under isothermal conditions at different temperatures (295, 297, 299, 301, 303, 305 and 307°K).

A Nikon microscope type S-ke attached to a Nikon camera M-35S, with a magnification of x 400, was placed in a temperature control chamber at a temperature (within ± 1°K) which was coincident with the DSC isothermal analysis. All equipment was held in the temperature control chamber until an equilibrium was reached at the desired temperature for observation. The experiment started when the melted oil sample (393°K for 5 min.) was dropped on the glass slide of the microscope within the control chamber. The sample thickness between the cover glass and the glass slide was kept between five to seven microns by using a constant thickness aluminum foil. The thickness was checked after each observation with a micrometer gauge.

The growth of the dendritic spherulites was measured photographically at regular intervals. Three determinations were made at each temperature. Five or more spherulites from different nucleation times were selected from the photographs, and their size was determined as an average of two crossed diameters in a constant direction. The relation between spherulite size and developing time was found to be parabolic. The linear growth rate of the spherulite at each isothermal crystallization temperature was then expressed as the slope of this parabolic curve during the initial phase of crystal growth.

## RESULTS AND DISCUSSION

### Polymorphic Behavior of Palm Oil

The effect of sample size on crystallization behavior was studied by varying sample quantities from ca. 3 mg to ca. 15 mg. It was found that 2-3 mg of sample was enough to cover the bottom surface of the standard pan (DSC-2). However, sample sizes of 3 to 15 mg had no significant effect on the isothermal crystallization and heating curves except for the thermal peak size. Therefore, a sample size of ca. 9 mg was chosen to apply for DSC studies in this experiment.

Some representative curves of DSC isothermal crystallization are shown in Figure 1. There are two exothermal

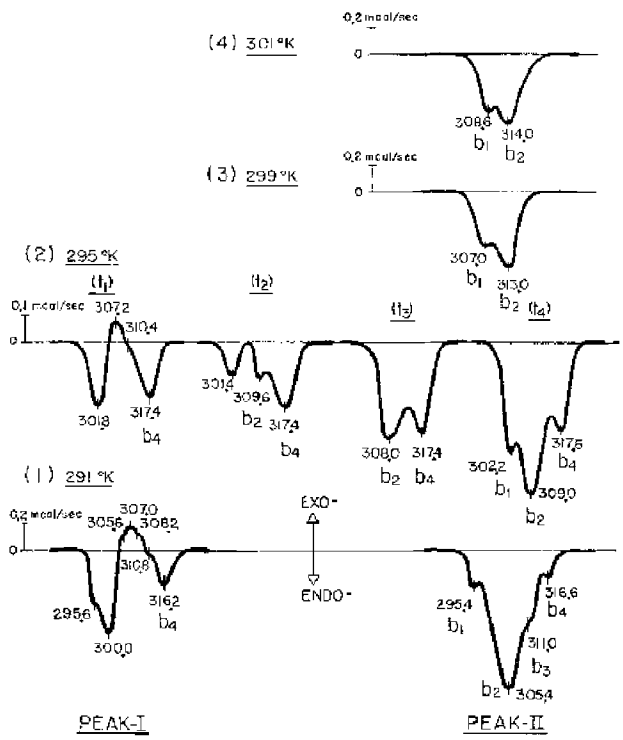


FIG. 2. DSC heating curves, samples cooled isothermally (shown in Fig. 1.) and heated at 10°K/min. 1) Sample cooled at 291°K. Left side: heating at a stage after peak -I. Right side: heating at a stage after peak -II. 2) Sample cooled at 295°K. Heating curves initiated at different stages ($t_1$ - $t_4$) in crystal development under isothermal condition. 3) Sample cooled at 299°K, after peak -II. 4) Sample cooled at 301°K, after peak -II.

TABLE II

Temperature of Endothermal Peak in Heating Curves vs. Crystallization Temperature, Samples Crystallized Isothermally after Peak -II (Fig. 1) and Heated at 10°K/Min

| Isothermal crystallization temperature | Peak-top temperature in heating curves (°K) | | | |
|---|---|---|---|---|
| °K | $b_1$ | $b_2$ | $b_3$ | $b_4$ |
| 291 | 295.4 | 305.4 | 311.0 | 316.6 |
| 293 | 298.4 | 307.0 | 311.0 | 316.6 |
| 295 | 302.2 | 309.0 | --- | 317.6 |
| 297 | 304.4 | 310.4 | --- | 318.0 |
| 299 | 307.0 | 313.0 | --- | --- |
| 301 | 308.6 | 314.0 | --- | --- |
| 303 | 311.2 | 316.4 | --- | --- |
| 305 | 313.4 | 322.0 | --- | --- |

peaks which can be easily distinguished at crystallization temperatures below 297°K, which are respectively termed peak-I and peak-II in order of generation in Figure 1-1. With increasing crystallization temperatures, the generation of both peaks is rapidly delayed, until finally peak-I disappears at temperatures of 299°K or higher. This is more obvious in Figure 1-2 which shows only peak-II appearing at temperatures of 299°K. and 301°K. The differences among isothermally quenched crystals can be identified in the DSC heating curves (at a rate of +10°K/min.) of Figure 2. The transition process under isothermal conditions is also shown in Fig. 2-2. These heating curves at the different stages of the isothermal crystallization were derived from the curve at 295°K (Fig. 1-1) at the indicated positions $t_1$, $t_2$, $t_3$ and $t_4$ corresponding to the development of peak-II.

The crystals of peak-I are transformed from the endothermal peaks at ca. 300 ~ 302°K to the endothermal peaks at ca. 316 ~ 318°K by the recrystallization at ca. 307°K under a heating condition of 10°K/min. (Fig. 2-1, -2 left side). If the heating rate is further increased to +40°K/min., the transformation is overcome by the rapid heating and the recrystallization does not occur. The only endothermal peak of peak-I crystals is shown at ca. 315°K in a heating curve of 40°K/min. Such crystals are tentatively termed A-form, which shows the endothermal peak at ca. 300 ~ 302°K in a heating curve of 10°K/min. or at ca. 315°K in a curve of 40°K/min.

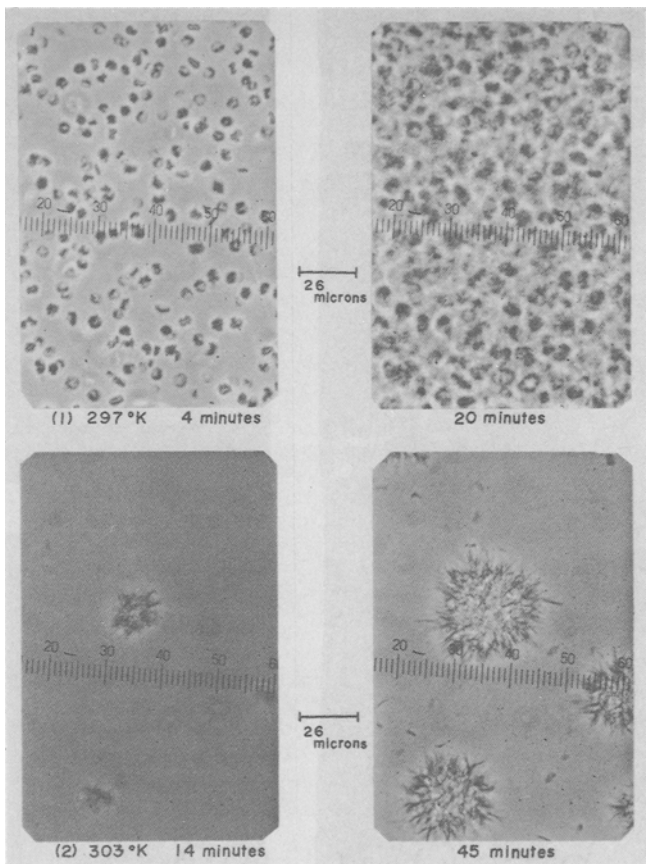


FIG. 3. Spherulite growth of palm oil under isothermal conditions 1) Isothermal crystallization temperature: 297°K, corresponding to the generation of peak -I and peak -II. 2) Isothermal crystallization temperature: 303°K, corresponding to the generation of peak-II.

The crystals resulting from the generation of peak-II are tentatively termed B-form. The right side of Figure 2 shows the heating curves at a rate of 10°K/min. after the generation of peak-II under isothermal conditions. For each isothermal crystallization temperature listed on Table II, these heating curves are composed of the endothermal peaks $b_1$, $b_2$, $b_3$ and $b_4$ in order of increasing peak temperatures. While $b_1$ and $b_2$ peaks are observed at all temperatures, only for isothermal crystallization temperatures below 297°K where both A and B forms are generated, are the endothermal peaks of $b_3$ and $b_4$, (or $b_4$ alone) observed. The peak temperatures of $b_3$ and $b_4$ are coincident with those of melting peaks of crystals which are transformed from A-form crystals at a heating rate of 10 K/min. Above 299°K, B-form crystals only show endothermal peaks of $b_1$ and $b_2$ in the heating curves and do not contain crystals derived from the A-form.

These different crystallizations (A-form and B-form) are also verified by microscopic observation, as shown in Figure 3. Below 297°K, dotted crystals occur very rapidly at first and then are gradually surrounded by different crystal-shaped-like tufts as in Figure 3-1. Above 299°K, there are

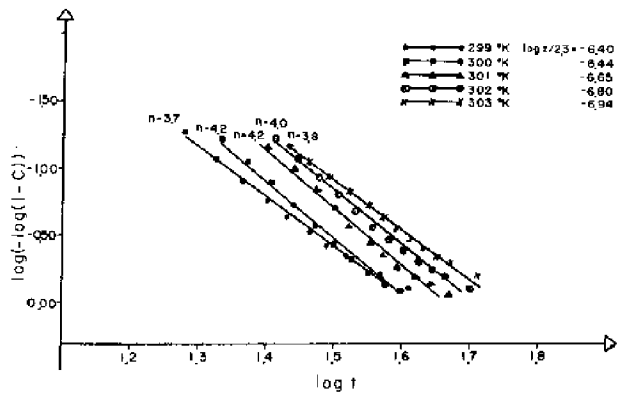


FIG. 4. Plot of palm oil crystallization using Avrami's equations (data collected from Figs. 1-2).

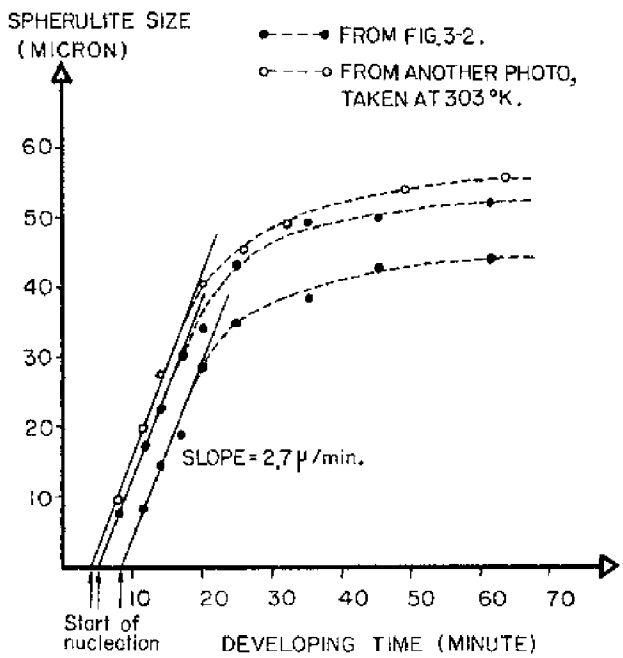


FIG. 5. The relation between spherulite size and developing time for B-form crystallization at 303°K. The spherulite growth rate (G) equals the slope of parabolic curve during the initial phase of crystal growth.

only dendritic spherulites and no dotted ones as in Fig. 3-2. Since these results coincide with DSC isothermal analysis, it appears that A-form crystals formed at the beginning of isothermal crystallization (at temperatures below 297°K) are related to the dotted spherulites, while B-form crystals formed during isothermal crystallization (at temperatures above 299°K) were related to the dendritic spherulites.

It has previously been determined by Sumi et al. (33) using an X-ray diffractometer that palm oil contains beta-form crystals after the crystallization at ambient temperature. Persmark et al. (34) has observed that palm oil contains alpha-form crystals during tempering after rapid quenching and subsequently beta prime-form crystals. Hoerr (16) has also previously observed that beta crystals grow to a size of several tens of microns while the alpha crystals are limited to ca. 5 microns in size. A-form and B-form crystals by DSC isothermal analysis appear to be coincident with alpha-form and beta-form respectively. But they might be contaminated with beta prime-form crystals in some cases. DSC studies of the polymorphic behavior of

TABLE III

Linear Growth Rate and Nucleation Rate of Spherulites in B-Form Crystals

| Temperature (T) | Linear growth rate (G) | Nucleation rate (I) |
|---|---|---|
| °K | Micron/Min | )/Min. $\mu^3$ |
| 299 | 3.3 | $2.4 \times 10^{-8}$ |
| 301 | 3.1 | $1.6 \times 10^{-8}$ |
| 303 | 2.7 | $1.3 \times 10^{-8}$ |
| 305 | 2.4 | — |
| 307 | 1.8 | — |

palm oil will be described in detail relative to alpha, beta-prime, and beta-form crystallization in a subsequent paper.

## Thermodynamic Analysis of Crystal Growth

B-form crystals are easily recognized as spherulite growth as they become much larger than A-form crystals. This difference can be used to advantage when applying Avrami's equation and calculating the linear growth rate of the spherulite.

The relation of the weight percentage of B-form crystals (C) and the time (t) is measured from the isothermal curves at 299°K to 303°K shown in Fig. 1-2. But the beginning ($C \leqslant 10\%$) and the ending stage ($C \geqslant 90\%$) are so greatly influenced by external factors that they must be disregarded for the calculation of Avrami's equation as is done in high polymer crystallization studies. The start of crystallization is defined as the point at which the exothermal curves rise from the base line. The period between the start of the system and the point of crystallization is also defined as the induction period where superficially there is no relation to the crystallization. These results are shown for n and log z/2.3 in Figure 4. The relationship between log (-log [1-C]) and log t is almost a straight line, the slope of which is near 4.0 at each crystallization temperature. That is, for the crystallization of B-form, the constant "n" of Avrami's equation is 4.0.

The linear growth rates calculated from the photomicrographs of dendritic spherulites are shown in Figure 5 and found to be the same at each given temperature and independent of the time of nucleation. The average rate (G) at each crystallization temperature is shown in Table III. In the case of microscopic observation, it is noticeable that the size of the B-form spherulites are finally several tens of microns greater than the thickness between the cover glass on the microscope slide. But the spherulite growth is not influenced by the sample thickness in such cases. This has been previously proven by Kamide (31) with isotactic polypropylene, by Takayanagi (24) with poly-(ethylene adipate) and by Flory et al. (35) with poly-(decamethylene sebacate). The oil sample under a microscope starts to nucleate more rapidly than in a DSC, even at the same crystallization temperature. That phenomenon seems to be caused by the different sample weight and configuration, and the different definition of the starting point.

The melting points of the oil crystals, which isothermally crystallized at different temperatures, are also defined from the DSC heating curves (10°K/min.) as the intersection of the base line and the tangent line of the endothermal peak as shown in Figure 6. Though palm oil is a mixture with different triglycerides, its specific heat can be assumed to be almost constant during crystallization in the same crystal form because they form a mixed crystal. The melting point of palm oil, since it is not a pure substance, is influenced by the temperature condition during crystallization and varies for given crystals as shown in Figure 6. Such a phenomenon was previously indicated by Falkai (36), and

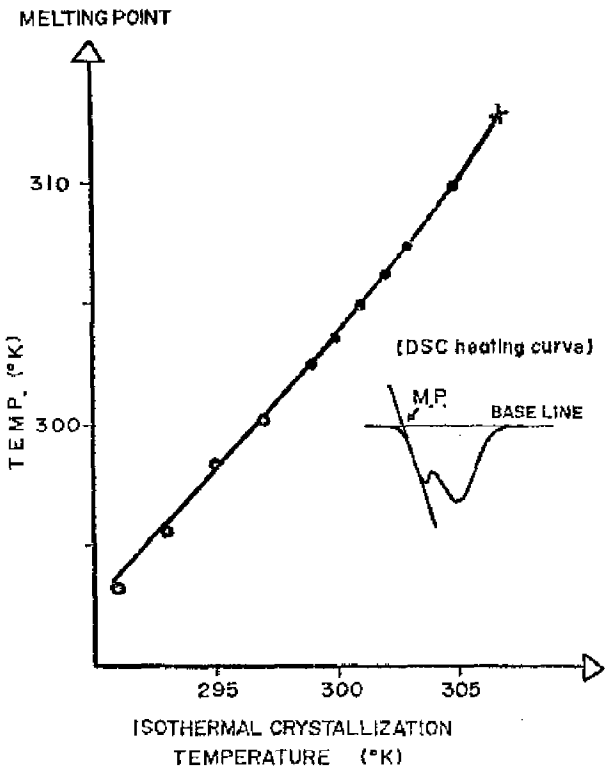


FIG. 6. Melting point of palm oil crystals quenched isothermally at different temperatures, from DSC heating curves. • – Melting point of B-form crystals; ○ - Melting point of B-form containing the transformed from A-form; X – Melting point is extrapolated from the trend of curve below 305°K. This point will be used for the calculation: the spherulite growth vs. supercooling in Fig. 7.

Jenkel and Wilsing (37) with high polymers like polypropylene. It implies that high molecular substances including fats and oils have no clear melting point but a melting range.

### Theoretical Study of Crystal Growth

The crystallization of palm oil (B-form) can be expressed as the process of nucleation and crystal growth from the studies of Mandelkern (22,23), Takayanagi (24-28) and Barnes (29). The dendritic spherulite growth can be considered as the formation of daughter crystals which are started by the surface nucleation and cover the surface of a parent crystal. In accordance with their teachings, the linear growth rate of spherulite (G) is controlled by surface nucleations which occur uniformly on parent crystals. Near the melting point (Tm), both the nucleation rate (I) and the linear growth rate (G) depend on the supercooling condition (Tm-T). If surface nucleation is three-dimensional, the logarithms of the growth rate (ln G) should be proportional to $Tm^2/(Tm-T)^2\ T$, or if two-dimensional, this term should be proportional to $Tm/(Tm-T)T$.

Since the linear growth rate (G) and the melting point (Tm) of B-form crystals in palm oil are determined by microscopy (Table III) and DSC studies (Fig. 6), respectively, the relationship between ln G and supercooling can be calculated for both cases: ln G vs. $Tm^2/(Tm-T)^2T$ or $Tm/(Tm-T)T$ at a temperature (T) as shown in Figure 7. It cannot be determined whether B-form crystals have two-dimensional nucleation or three-dimensional, because the experiment is restricted to a very narrow range of temperature (299-307°K) by the DSC. The ln G term appears to be proportional to both terms of $Tm^2/(Tm-T)^2T$ and $Tm/(Tm-T)T$.

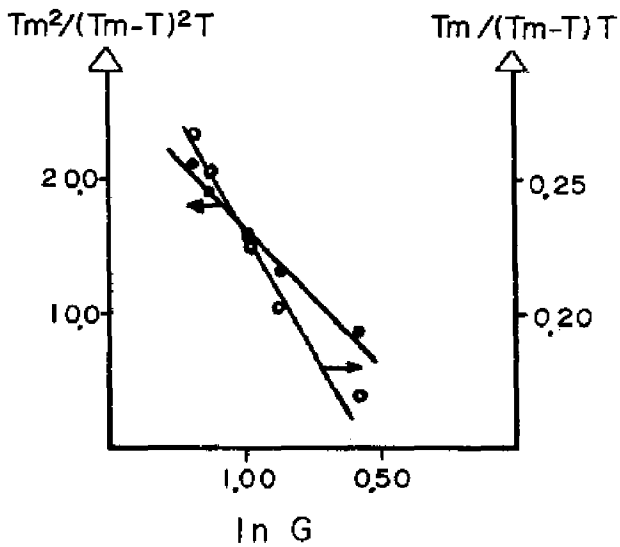


FIG. 7. Supercooling (Tm-T) vs. Linear growth rate of spherulite (ln G).

Avrami's theory can be rearranged to apply to B-form crystals of palm oil. The crystallization mechanism of this crystal form is found to be composed of homogeneous nucleation and polyhedral growth, because this sample (passed through a membrane filter) does not contain foreign particles and the constant "n" of Avrami's equation equals 4 (as stated earlier). The nucleation of this crystal form is also found to be sporadic in time, because the crystal growth rate is the same at a given temperature and independent of the time of nucleation as shown in Figure 5 and Table III.

The rate constant of crystallization "z" of Avrami's equation is a function of both the nucleation rate (I) and the linear growth rate (G) as shown in Table I. Theoretically, this constant (z) appears to be dominated by the supercooling condition near the melting point as well as the terms I and G. When the constant "z" can be derived from measurements with a DSC (Fig. 4) and the rate "G" from the spherulite growth determined by microscopy (Table III), the nucleation rate (I) can be calculated for each crystallization temperature using the equation in Table I. Such results are shown in Table III. Thus, even though it is generally hard to investigate the nucleation rate with microscopy for such high molecular substances, the nucleation rate can be obtained using one of Avrami's equations in Table I.

From this work the DSC isothermal analysis has been shown to be quite useful not only for the investigation of the polymorphism, but also for investigating the kinetics of crystallization.

ACKNOWLEDGMENTS

The author thanks J.M. Hasman, C.M. Jansen, and A.E. Waltking for their technical advice and review of this paper. He also thanks K. Hiratsuka, president of Knorr Foods Co., Ltd., Japan, for his support of this research. This investigation was partially completed at Knorr Foods Co., Ltd., Japan (CPC International Inc.).

REFERENCES

1. Hannewijk, J., and A.J. Haighton, JAOCS 35:3457 (1958).
2. Merker, D.R., L.C. Brown, and L.H. Wiedermann, Ibid. 35:130 (1958).
3. Wilton, I., "Fat and Oil Chemistry," Proceedings of the 4th. Scandinavian Symposium of Fats and Oils, p. 95 (1966).
4. Hoerr, C.W., and F.R. Paulicka, JAOCS 45:793 (1968).

5. Chapman, G.M., Ibid. 48:824 (1971).
6. Luddy, F.E., J.W. Hampson, S.F. Herb, and H.L. Rothbart, Ibid. 50:240 (1973).
7. Rossell, J.B., Ibid. 52:505 (1975).
8. Hagemann, J.W., and W.H. Tallent, Ibid. 52:204 (1975).
9. Lovegren, N.V., H.S. Gray, and R.O. Feuge, Ibid. 53:83 (1976).
10. Dafler, J.R., Ibid. 54:249 (1977).
11. Sone, T., J. Phys. Soc. Jpn. 16:961 (1961).
12. Loeser, E., Fette Seif. Anstrichm. 73:262 (1972).
13. Larsson, K., Acta Chem. Scand. 20:2255 (1966).
14. Larsson, K., Chem. Scr. 1:21 (1971).
15. Larsson, K., Fette Seif. Anstrichm. 74:136 (1972).
16. Hoerr, C.W., JAOCS 37:539 (1960).
17. Avrami, M., J. Chem. Phys. 7:1103 (1939).
18. Avrami, M., Ibid. 8:212 (1940).
19. Avrami, M., Ibid. 9:177 (1941).
20. Evans, U.R., Trans. Faraday Soc. 41:365 (1945).
21. Volmer, M., and A. Weber, Z. Phys. Chem. 119:227 (1925).
22. Mandelkern, L., F.A. Quinn, and P.J. Flory, J. Appl. Phys. 25:830 (1954).
23. Mandelkern, L., Chem. Revs. 56:903 (1956).
24. Takayanagi, M., T. Yamashita, and K. Saheki, J. Ind. Chem. Jpn. 60:299 (1957).
25. Takayanagi, M., and S. Kuriyama, Ibid. 57:873 (1954).
26. Takayanagi, M., M. Nakao, and K. Machida, Ibid. 59:549 (1956).
27. Takayanagi, M., and T. Yamashita, Ibid. 60:456 (1957).
28. Takayanagi, M., and T. Kusumoto, Ibid. 62:587 (1959).
29. Barnes, W.J., W.G. Luetzel, and F.P. Price, J. Phys. Chem. 65:1742 (1961).
30. Kamide, K., and K. Fujii, Polym. Chem. Jpn. 25:155 (1968).
31. Kamide K., Chem. High Polymers Jpn. 24:259 (1967).
32. "Official and Tentative Methods of the American Oil Chemists' Society," Vol. I, AOCS, Champaign, IL, 1964, (revised 1975), Method Ce 1–62.
33. Sumi, K., and Y. Abe, J. Jpn. Oil Chem. Soc. 14:606 (1965).
34. Persmark, U., K.A. Melin, and P.O. Stahl, Riv. Ital. Del. Sos. Gra. LIII:301 (1976).
35. Flory, P.J., and A.D. McIntyre, J. Polym. Sci. 18:592 (1955).
36. Falkai, B.V., Makromol. Chem. 41:86 (1960).
37. Jenckel, E., and H. Wilsing, Z. Elektrochem. Angew. Physik Chem. 53:4 (1949).

[Received December 15, 1978]